ELSEVIER

The molecular structure of $[In(P_3C_2Bu_2^t)]$ using gas-phase electron diffraction and *ab initio* and DFT calculations

Derek A. Wann [a], Sarah L. Hinchley [a], Heather E. Robertson [a], Matthew D. Francis [b], John F. Nixon [b], David W.H. Rankin [a,*]

[a] *School of Chemistry, University of Edinburgh, West Mains Road, Edinburgh EH9 3JJ, UK*
[b] *Department of Chemistry, School of Life Sciences, University of Sussex, Falmer, Brighton BN1 9QJ, UK*

Abstract

The molecular structure of $[In(P_3C_2Bu_2^t)]$ has been determined by gas-phase electron diffraction using the SARACEN method. The experimental geometric parameters showed good correlation with those obtained from quantum chemical calculations and from a previous X-ray diffraction study. Calculations were performed using various DFT methods and also MP2 theory to identify the most suitable method for calculating structures of this type. The accuracy of the calculations was gauged by reference to experimentally determined parameters. The use of small-core and large-core pseudopotentials on the indium atom was also tested, showing that the lack of electrons explicitly considered in the calculation when a large-core pseudopotential was used affected the accuracy of the calculation. Similar calculations have been performed for the less symmetrical $[In(P_2C_3Bu_3^t)]$, but electron diffraction data of adequate quality could not be obtained.
© 2006 Elsevier B.V. All rights reserved.

1. Introduction

In the past 20 years, many unsaturated ring systems have been synthesised using the phospha-alkyne synthon, $Bu^tC{\equiv}P$ [1]. A selection of these rings is shown in Fig. 1.

Complexes in which $[P_3C_2Bu_2^t]^-$ and $[P_2C_3Bu_3^t]^-$ have been coordinated to d- and f-block metals have been studied extensively [2], but until 1999 little was known about similar complexes with main-group elements. Singly charged anions such as $[P_3C_2Bu_2^t]^-$ and $[P_2C_3Bu_3^t]^-$ are of interest because of their ability to stabilise monovalent metals. Complexes with the Group 13 metals Ga, In and Tl have been synthesised [3–5] and have potential uses in the manufacture of III–V semiconductors. The indium complexes $[In(P_3C_2Bu_2^t)]$, **1**, and $[In(P_2C_3Bu_3^t)]$, **2**, contain

both precursor atoms for the formation of indium phosphide and their volatility could lend themselves to use in chemical vapour deposition (CVD) of semiconducting films [6].

Compounds **1** and **2** have both previously been studied using X-ray diffraction [4,5], and both crystal structures showed In coordinated to the ring in an η^5-fashion. However, while the crystal structure of **2** consisted of distinct monomers, the structure of **1** displayed weakly bound chains of molecules. The reason for this difference was explained by the increased steric bulk of **2**, with an extra Bu^t group attached to the ring. This phenomenon is further observed in the crystal structure of $[In(\eta^5\text{-}C_5H_4Bu^t)]$, in which the presence of less steric bulk allows the In-centroid distances between an indium atom and the two adjacent rings to be as similar as 253 and 285 pm [7]. The values for the In-centroid distances in the crystal structure of **1** are 259.8 pm to the strongly associated ring and 352.6 pm

---
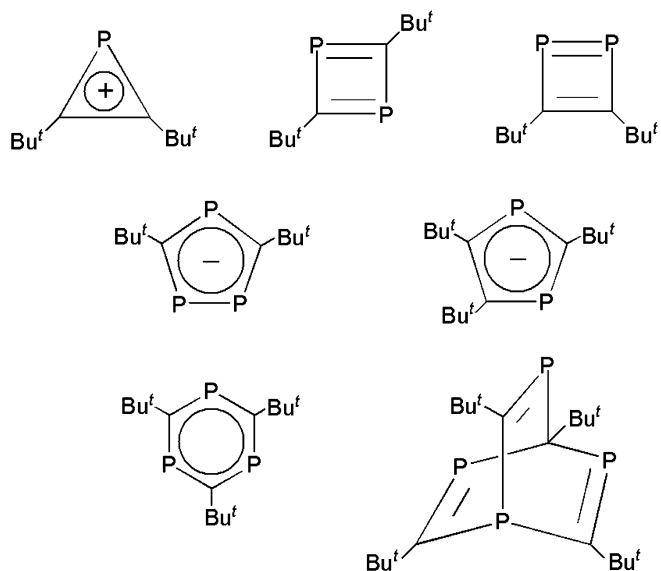
Fig. 1. A selection of unsaturated rings that can be synthesised from $Bu^tC{\equiv}P$.

to the next ring in the chain, thus demonstrating weak aggregation.

This paper describes a search for suitable *ab initio* and DFT methods for performing calculations on Group 13 half-sandwich complexes and the use of calculated parameters during the GED structure determination of $[In(P_3C_2Bu^t_2)]$, **1**.

2. Experimental

2.1. Synthesis

Samples of **1** and **2** were prepared by the co-condensation of indium vapour and $Bu^tC{\equiv}P$ at 77 K or by treatment of indium(I) iodide with the corresponding potassium salts of the $P_3C_2Bu^t_2$ and $P_2C_3Bu^t_3$ ring anions, according to the literature methods [4,5].

2.2. Theoretical methods

The calculations reported in this work were performed using the GAUSSIAN 03 suite of programs [8], with the resources of the EPSRC National Service for Computational Chemistry Software. Some of the calculations were carried out using a cluster of six HP ES40 computers, where each Alphaserver ES40 machine has four 833 MHz EV68 CPUs and 8 GB of memory connected with a high-speed, low-latency QSW switch forming an Alphaserver SC. Other calculations were performed using a cluster of 22 Linux Opteron nodes. Each Opteron server has twin 2.4 GHz Opteron 250 CPUs and 8 GB of memory connected with a high-speed, low-latency Myrinet network.

The starting coordinates for the geometry optimisation calculation for **1** were taken from the structure obtained by X-ray diffraction [4]. C_s symmetry was imposed and calculations were initially performed at the Hartree–Fock

level of theory using first the 3-21G* basis set [9] and then the 6-31G* basis set [10] on the light atoms (H, C and P) and the LanL2DZ basis set [11], including an effective core potential (ECP), on the indium atom. When geometry optimisations were performed at these levels, it was noted that the calculations had difficulty in reaching convergence as the forces acting on the atoms became too small. This is characteristic of a very shallow potential-energy surface (PES). Force fields were calculated at these levels and showed that there was a single imaginary frequency ($\sim 13i\ cm^{-1}$), indicating that a minimum on the PES had not been reached. By visualising the imaginary frequency using the MOLEKEL graphics program [12], it was seen that the frequency was associated with the twists of the symmetry-related *tert*-butyl groups. A modified geometry optimisation was performed using the direct inversion in the iterative subspace (GDIIS) algorithm [13], as this is known to aid convergence of calculations of large molecules, especially those having a shallow PES.

Calculations were also performed at different levels of theory, namely BLYP [14,15], B3LYP [15,16], B3PW91 [16,17] and MP2 [18]. A scan of the PES was performed (B3PW91/LanL2DZ/6-31G*) to gain an insight into its form (Fig. 2). The torsional angle C(9)–C(7)–C(3)–P(2) was varied in steps of $5°$ from a zero-torsion position, where the C_{tert}–C_{Me} bond was eclipsing the C(3)–P(2) ring bond. (See Fig. 3 for atom numbering.) When the calculations were started from a position where the C(9)–C(7)–C(3)–P(2) torsion angle was $40°$, a structure with real frequencies was obtained, indicating that the optimised geometry represented an energy minimum.

The LanL2DZ pseudopotential that was used above is an example of a large-core ECP. For the indium atom, LanL2DZ considers 46 of the 49 electrons to belong to the electronic core. Recently, small-core pseudopotentials were developed that regard only 28 of the electrons to be in the core ([Ar] + 4d) and treat the rest explicitly. A quadruple-ζ basis set of this type [19] (aug-cc-pVQZ-PP) has been tested to see whether the inclusion of more electrons in the valence
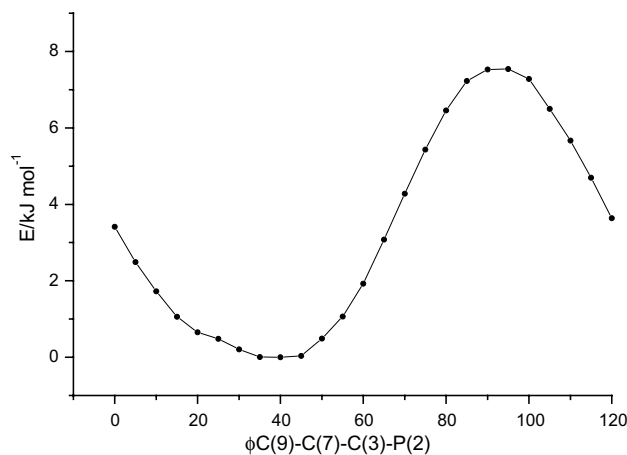

Fig. 2. Relative energies upon rotation about the C_{ring}–C_{tert} bond in $[In(P_3C_2\ Bu^t_2)]$, **1**.
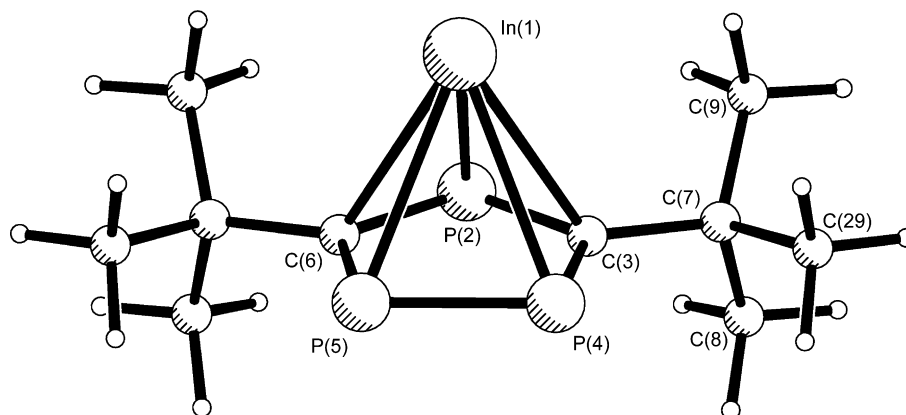
Fig. 3. Structure of $[In(P_3C_2Bu_2^t)]$, **1**, with C_s symmetry, showing the atom numbering used in calculations and the GED refinement.

shell of the atom can produce more reliable theoretical structures. The accuracy of each method will be assessed by comparison with the GED structure for **1**.

A similar set of calculations was performed for **2**. Again, different methods were tried and a variety of pseudopotentials was used. Unlike **1**, molecule **2** was found to have C_1 symmetry.

An analytical force field was calculated at the RHF/aug-cc-pVQZ-PP/6-31G* level for **1** and was used with the SHRINK program [20] to calculate accurate amplitudes of vibration (u_{h1}) and curvilinear corrections (k_{h1}) to allow for the shrinkage effects that are associated with the GED experiment [21].

2.3. Gas-phase electron diffraction

Data were collected for **1** using the Edinburgh gas-phase electron diffraction apparatus [22]. A voltage of approximately 40 kV was used to accelerate the electrons, resulting in an electron wavelength of around 6.0 pm. The intensities of the scattered electrons were recorded using Kodak Electron Image films. Data were collected for **1** at a nozzle-to-film distance of 254.05 mm with sample and nozzle temperatures of 481 and 487 K, respectively. Unfortunately, to obtain shorter nozzle-to-film data would require heating of the sample beyond the current capabilities of the GED apparatus, with the increased risk of thermal decomposition.

The weighting points for the off-diagonal weight matrices, correlation parameters and scale factors for both sets of data are given in Table S1 in Supplementary material. Also included are the wavelengths of the electrons as determined from the scattering patterns for benzene, which were recorded immediately after the pattern for compound **1**. The scattering intensities were measured using an Epson Expression 1600 Pro flatbed scanner and converted to mean optical densities as a function of the scattering variable, s, using an established program [23]. The data reduction and least-squares refinement process was carried out using the ed@ed program [24], employing the scattering factors of Ross et al. [25].

3. Results and discussion

A large amount of work has previously been directed towards calculating the structures of transition-metal complexes incorporating ring systems. A review [26] of the computational chemistry of metallocenes investigated the application of *ab initio* and DFT methods to the modelling of transition-metal complexes and in particular ferrocene. It concluded that, in general, DFT methods could reproduce geometries for transition-metal complexes much more accurately than MP2 calculations.

Previous work on a Group 14 complex $[Sn(P_2C_2Bu_2^t)]$ found that a hybrid DFT method (B3PW91) gave geometries that were close to the GED structure [27] and here we further test suitable computational methods. As part of the structure determination of the Group 13 half-sandwich complex $[In(P_3C_2Bu_2^t)]$, **1**, several DFT methods as well as MP2 have been tested for their ability to calculate accurate geometries for this class of compound. The use of both small-core (aug-cc-pVQZ-PP) and large-core (LanL2DZ) ECPs has also been investigated. Calculations were also performed for the associated complex $[In(P_2C_3Bu_3^t)]$, **2**. Selected parameters from these geometry optimisations are given in Table 1. See Figs. 3 and 4 for the atom numbering of **1** and **2**, respectively.

For **1**, the calculations that most closely matched the GED experimental results were those performed using the B3PW91 method with the small-core ECP on indium. The parameters were chosen for comparison because they were defined by the GED experiment without the need for restraints, which themselves are derived from calculated values. Using the LanL2DZ ECP with this method overestimated the In-ring distances by between 1 and 3 pm. For MP2, neither the large-core nor the small-core ECPs gave results concordant with those from experiment. Although MP2/LanL2DZ calculated rIn–C to within 1.5 pm of the GED value, rIn–P was overestimated by up to 8 pm. Similarly, poor results were obtained for the B3LYP and BLYP methods, which overestimated bond lengths by between 6 and 11 pm for rIn–P(2), and by between 5 and

Table 1
Selected parameters from the structures of **1** and **2** determined by experimental and theoretical methods[a]

	XRD[b,c]	GED	MP2		B3PW91		B3LYP		BLYP		PW91PW91		PBE1PBE	
1			SC	LC	SC	LC	SC	LC	SC	LC	SC	LC	SC	LC
rIn–P(2)	310.8(4)	293.5(20)	301.9	296.8	294.6	296.0	300.2	300.6	304.4	303.7	296.0	297.1	292.9	295.1
rIn–P(4/5)	303.5(3)	292.7(14)	298.8	300.3	293.1	296.3	297.7	299.9	301.0	302.0	294.4	297.0	291.8	295.4
rIn–C	298.1(9)	283.2(10)	290.8	281.9	283.0	284.0	288.4	288.5	292.5	291.5	284.0	284.5	281.1	282.6
rP(2)–C(3/6)	178.1(10)	177.1(4)	175.7	176.5	176.6	176.6	177.2	177.2	179.0	179.0	177.9	177.9	176.3	176.3
rP(4/5)–C(3/6)	174.8(10)	176.5(4)	174.3	177.0	176.0	176.0	176.6	176.5	178.5	178.5	177.4	177.4	175.7	175.7
rP–P	211.1(5)	213.2(11)	212.8	212.7	214.2	214.0	215.3	215.1	218.0	217.9	215.9	215.7	213.6	213.3
∠C_{ring}–P–C_{ring}	100.0(7)	100.3(5)	101.3	99.3	100.3	100.0	100.6	100.3	100.7	100.3	100.1	99.8	100.2	99.9
∠P–C_{ring}–P	119.8(6)	120.3(4)	119.6	121.0	120.5	120.7	120.3	120.5	120.4	120.6	120.7	121.0	120.6	120.8
∠C_{ring}–P–P	100.2(3)	99.6(2)	99.7	99.2	99.3	99.3	99.4	99.3	99.3	99.2	99.2	99.1	99.3	99.2
2			SC[d]	LC[d]	SC	LC	SC	LC	SC	LC	SC	LC	SC	LC
rIn–P	290.8(3)	–	–	–	285.4	288.0	290.2	290.6	294.4	293.0	287.5	288.7	285.0	287.0
rIn–C(2)	281.1(9)	–	–	–	275.7	277.2	280.0	280.1	283.8	282.5	277.1	277.9	274.2	276.3
rIn–C(4/5)[e]	283.5(9)	–	–	–	277.3	278.6	284.3	282.8	288.5	285.7	279.9	279.4	276.8	277.4
rP(3/6)–C(2)[e]	172.8(9)	–	–	–	174.8	174.8	175.3	175.2	177.0	177.0	176.1	176.0	174.5	174.5
rP(3/6)–C(4/5)[e]	178.9(10)	–	–	–	180.8	180.7	181.7	181.5	183.7	183.5	182.1	182.0	180.3	180.2
rC$_{ring}$–C$_{ring}$	142.9(11)	–	–	–	141.7	141.8	141.8	141.9	142.9	143.0	142.5	142.5	141.5	141.6
∠C_{ring}–C_{ring}–P[e]	114.9(7)	–	–	–	115.1	115.2	115.1	115.1	115.1	115.1	115.2	115.3	115.2	115.2
∠P–C_{ring}–P	116.3(5)	–	–	–	115.2	115.4	115.0	115.2	115.1	115.3	115.5	115.7	115.3	115.5
∠C_{ring}–P–C_{ring}[e]	97.0(4)	–	–	–	97.3	97.1	97.4	97.3	97.4	97.2	97.0	96.8	97.2	97.0

For each of the theoretical methods both a small-core aug-cc-pVQZ-PP (SC) and large-core LanL2DZ (LC) pseudopotential have been tested on the indium atom.

[a] Distances (r) are in pm, angles (∠) in °.
[b] Values for **1** taken from Ref. [4].
[c] Values for **2** taken from Ref. [5].
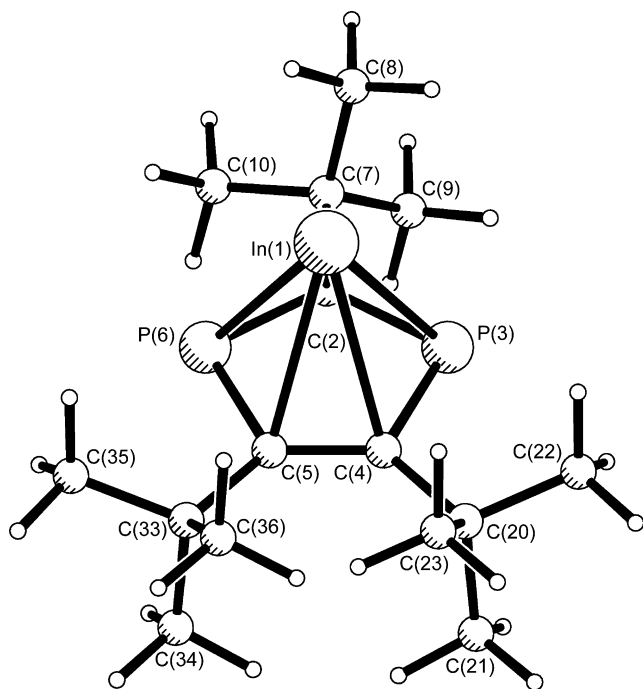[d] MP2 calculations proved too computationally demanding for **2**.
[e] Average value.

Fig. 4. Structure of $[In(P_2C_3Bu^t_2)]$, **2**, with C_1 symmetry showing the atom numbering used in calculations.

9 pm for both rIn–P(4/5) and rIn–C. The PW91PW91 and PBE1PBE methods performed better, generally predicting distances to within a few picometres, especially when using

the small-core ECP. Coordinates for each of the calculated geometries are given in Tables S2–S13.

$[In(P_2C_3Bu^t_3)]$, **2**, has more atoms (and therefore more electrons) than **1** and is also of lower symmetry. For these reasons similar calculations for **2** took longer and required more CPU memory. In fact, despite the powerful resources of the NSCCS Opteron clusters, it proved impossible to run MP2 calculations for **2**. As it was not possible to collect meaningful GED data for **2**, no comparison can be made between the calculated structure and that in the gas phase. The calculated results do, however, show a degree of correlation with the parameters obtained from X-ray diffraction [5]. Ideally, calculated parameters should be compared with gas-phase data, where structures are not altered by packing forces, but on this occasion some comparisons will be made with the crystal structure. This course of action is supported by the nature of the crystal structure of **2**. Unlike **1**, for which chains of molecules were observed in the crystalline phase [4] and, consequently, the In-ring distances are much longer than the gas-phase distances (Table 1), the molecules of **2** in the crystal are further apart, minimising intermolecular interactions. Thus the molecular structures in the gas phase and solid state will be more similar.

In the case of **2**, the B3LYP calculations give In-ring bond lengths that are within about 1 pm of those determined by X-ray diffraction. Here, the use of the small-core and large-core basis sets makes less difference to the parameters, with most bond lengths lying within 2 pm of one

another. As was found for **1**, the BLYP method overestimated most distances and the PW91PW91 and PBE1PBE methods underestimated them. For **1**, there was a definite trend towards the use of small-core ECPs giving more accurate results. Such a trend is not observed for **2**, where sometimes the use of a small-core ECP gives a result closer to the experimental value and sometimes further away. Coordinates for each of the calculated geometries are given in Tables S14–S23.

The SARACEN method [28] was used to determine the structure of $[In(P_3C_2Bu_2^t)]$, **1**. A C_s-symmetry model was written describing the molecule as a planar ring with an attendant indium atom, which was free to move above the ring within the constraints of C_s symmetry. The two *tert*-butyl groups were related through symmetry and were allowed to bend out of the plane of the ring. In total the geometry was described by 11 distance parameters, seven angle parameters and two torsion angle parameters (see Table 2). The distances included a single C–H bond length (p_1) as the theoretical structure (B3PW91/aug-cc-pVQZ-PP/6-311+G*) showed all the distances to be within 0.2 pm of one another. The four different C–C bond lengths

Table 2
Refined (r_{h1}) and calculated (r_e) geometric parameters for $[In(P_3C_2Bu_2^t)]$, **1**, from the GED study using SARACEN[a,b]

Parameter		r_{h1}	r_e	Restraint
Independent				
p_1	rC–H mean	109.6(4)	109.5	109.5(5)
p_2	rC–C average	154.1(3)	154.9	–
p_3	rC–C difference 1	0.3(1)	0.3	0.3(1)
p_4	rC–C difference 2	−0.2(1)	−0.2	−0.2(1)
p_5	rC–C difference 3	0.6(2)	0.6	0.6(2)
p_6	rC–P average	176.8(3)	176.3	–
p_7	rC–P difference	0.6(2)	0.6	0.6(2)
p_8	rP–P	213.2(11)	214.2	–
p_9	rC(3)···C(6)	272.0(10)	271.3	–
p_{10}	rIn–P(2)	293.5(20)	294.6	–
p_{11}	rIn–C(3/6)	283.2(10)	283.0	–
p_{12}	$\angle$C$_{ring}$–C$_{tert}$–C$_{Me}$ average	111.2(6)	110.3	–
p_{13}	$\angle$C$_{ring}$–C$_{tert}$–C$_{Me}$ difference 1	2.7(6)	2.1	2.1(7)
p_{14}	$\angle$C$_{ring}$–C$_{tert}$–C$_{Me}$ difference 2	−4.5(7)	−4.3	−4.3(8)
p_{15}	$\angle$C$_{Me1}$–C$_{tert}$–C$_{Me3}$	108.0(10)	108.8	108.2(10)
p_{16}	$\angle$C$_{Me2}$–C$_{tert}$–C$_{Me3}$	108.5(10)	108.7	108.9(10)
p_{17}	$\angle$C$_{tert}$–C$_{Me}$–H mean	111.5(10)	111.1	111.1(10)
p_{18}	$\angle$P(2)–C$_{ring}$–C$_{tert}$	120.5(11)	119.3	–
p_{19}	ϕBu^t	48.4(50)	34.0	–
p_{20}	ϕP(5)–P(4)–C(3)–C(7)	3.4(5)	3.3	3.3(5)
Dependent				
p_{21}	rIn–P(4/5)	292.7(14)	293.1	–
p_{22}	rC(6/3)–P(2)	177.1(4)	176.6	–
p_{23}	rC(3/6)–P(4/5)	176.5(4)	176.0	–
p_{24}	$\angle$C$_{ring}$–P–C$_{ring}$	100.3(5)	100.3	–
p_{25}	$\angle$P–C$_{ring}$–P	120.3(4)	120.5	–
p_{26}	$\angle$C$_{ring}$–P–P	99.6(2)	99.3	–

[a] Refers to B3PW91/aug-cc-pVQZ-PP/6-311+G*.
[b] Distances (r) are in pm, angles ($\angle$) and torsional angles (ϕ) in °. See text for parameter definitions and Fig. 3 for atom numbering. The figures in parentheses are the estimated standard deviations of the last digits. Me1 is the methyl group surrounding C(9), Me2 is associated with C(8) and Me3 with C(29).

were described by the average and three difference parameters according to the following equations, where Me1 is the methyl group containing C(9), Me2 contains C(8) and Me3 contains C(29) (see Fig. 3 for atom numbering):

$$p_2 = [r(C_{ring}–C_{tert}) + r(C_{tert}–C_{Me1}) + r(C_{tert}–C_{Me2})$$
$$+ r(C_{tert}–C_{Me3})]/4$$
$$p_3 = r(C_{ring}–C_{tert}) − \{[r(C_{tert}–C_{Me1}) + r(C_{tert}–C_{Me2})$$
$$+ r(C_{tert}–C_{Me3})]/3\}$$
$$p_4 = r(C_{tert}–C_{Me1}) − \{[r(C_{tert}–C_{Me2}) + r(C_{tert}–C_{Me3})]/2\}$$
$$p_5 = r(C_{tert}–C_{Me2}) − r(C_{tert}–C_{Me3})$$

Parameters 2–5 were then used to define the four C–C distances.

The two C–P bond lengths were described using the average of the two and the difference between them ($p_{6–7}$) and rP–P, which only appears once in the molecule, was p_8. The other distance used to describe the ring was the non-bonded C···C distance (p_9). In order to position the indium atom above the ring, rIn–P(2) and rIn–C$_{ring}$ were included as independent parameters ($p_{10–11}$).

The three different C$_{ring}$–C$_{tert}$–C$_{Me}$ angles were described using (i) the average of the three, (ii) the angle to Me1 minus the mean of the other two, and (iii) the difference between the angles to Me2 and Me3 ($p_{12–14}$). The angles between the methyl groups, which were needed to describe the asymmetry of the Bu^t groups fully, were defined as $\angle$C$_{Me1}$–C$_{tert}$–C$_{Me3}$ (p_{15}) and $\angle$C$_{Me2}$–C$_{tert}$–C$_{Me3}$ (p_{16}) and a single $\angle$C$_{tert}$–C$_{Me}$–H angle was used (p_{17}). Calculations (B3PW91/aug-cc-pVQZ-PP/6-311+G*) showed that the twist of each methyl group (*i.e.* the torsional angle formed by one C–H and C$_{ring}$–C$_{tert}$) was approximately 180° and these values were not allowed to vary in the final refinement.

$\angle$P(2)–C$_{ring}$–C$_{tert}$ (p_{18}) determined the angle that the Bu^t groups made with the P(2)–C(3) bond. The dihedral angle providing the twist of the Bu^t groups (applied so that C_s symmetry was preserved) was defined as ϕP(2)–C(3)–C(7)–C(9) (p_{19}), where the zero-torsion position has C(7)–C(9) eclipsing P(2)–C(3). A positive value for p_{19} relates to a twist of the Bu^t group containing C(7) in a clockwise direction when viewed from C(3) to C(7) and a twist in the opposite direction for the other Bu^t group. ϕP(5)–P(4)–C(3)–C(7) (p_{20}) allowed the Bu^t groups to bend out of the plane of the ring in the opposite direction to In.

In total, 20 geometric parameters and nine groups of amplitudes of vibration were refined during the least-squares refinement process. See Table S24 for a list of the amplitudes of vibration. Flexible restraints were employed, using the SARACEN method, for 11 geometric parameters and six amplitudes. The restraints were derived from calculations performed using B3PW91/aug-cc-pVQZ-PP/6-311+G*, which had proved the most accurate of the methods tested for determining this structure.

The success of the refinement, for which $R_G = 0.059$ ($R_D = 0.043$), can be gauged on the basis of the radial-distribution and experimental – theoretical difference
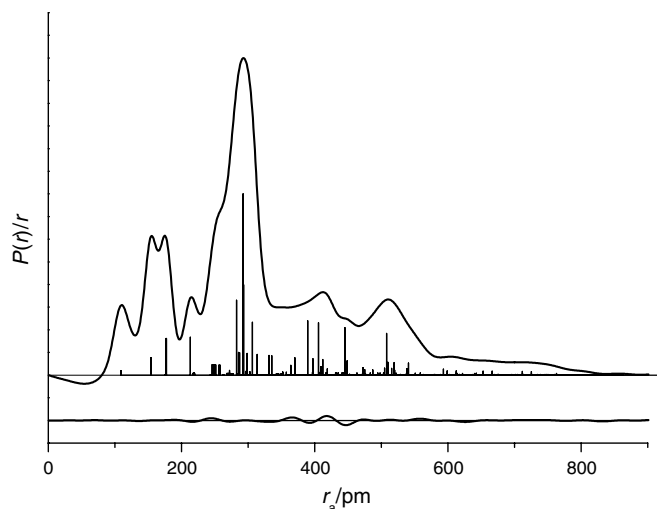
Fig. 5. Experimental and difference (experimental – theoretical) radial-distribution curves for $[In(P_3C_2Bu^t_2)]$, **1**. Before Fourier inversion, the data were multiplied by $s \cdot \exp(-0.00002s^2)/(Z_{In} - f_{In})(Z_C - f_C)$.

curves (Fig. 5) and the molecular-scattering intensity curve (Fig. S1). The least-squares correlation matrix is given in Table S25 and the coordinates for the GED structure are given in Table S26.

In conclusion, the calculated geometry for $[In(P_3C_2Bu^t_2)]$, **1**, using the B3PW91 method with a small-core aug-cc-pVQZ-PP ECP on indium, was very close to the geometry obtained from the GED refinement. The calculations also showed that it is advisable to use a small-core ECP wherever it is available as this can have a striking effect on the accuracy of *ab initio* and DFT calculations. It is unfortunate that, due to its lower volatility, it was not possible to extend this study to show that the same method of calculation is as good for $[In(P_2C_3Bu^t_3)]$, **2**.

Acknowledgements

Appendix A. Supplementary material

Supplementary data associated with this article can be found, in the online version, at doi:10.1016/j.jorganchem.2006.11.025.

References

[1] K.B. Dillon, F. Mathey, J.F. Nixon, Phosphorus: The Carbon Copy: From Organophosphorus to Phospha-organic Chemistry, John Wiley and Sons, Chichester, 1998, and references therein.
[2] J.F. Nixon, Coord. Chem. Rev. 145 (1995) 201.
[3] M.D. Francis, P.B. Hitchcock, J.F. Nixon, H. Schnöckel, J. Steiner, J. Organomet. Chem. 646 (2002) 191.
[4] A. Schnepf, G. Stößer, D. Carmichael, F. Mathey, H. Schnöckel, Angew. Chem., Int. Ed. Engl. 38 (1999) 1646.
[5] C. Callaghan, G.K.B. Clentsmith, F.G.N. Cloke, P.B. Hitchcock, J.F. Nixon, D.M. Vickers, Organometallics 18 (1999) 793.
[6] G.K.B. Clentsmith, F.G.N. Cloke, M.D. Francis, J.C. Green, P.B. Hitchcock, J.F. Nixon, J.L. Suter, D.M. Vickers, J. Chem. Soc., Dalton Trans. (2000) 1715.
[7] O.T. Beachley Jr., J.F. Lees, R.D. Rogers, J. Organomet. Chem. 418 (1991) 165.
[8] M.J. Frisch, G.W. Trucks, H.B. Schlegel, G.E. Scuseria, M.A. Robb, J.R. Cheeseman, J.A. Montgomery Jr., T. Vreven, K.N. Kudin, J.C. Burant, J.M. Millam, S.S. Iyengar, J. Tomasi, V. Barone, B. Mennucci, M. Cossi, G. Scalmani, N. Rega, G.A. Petersson, H. Nakatsuji, M. Hada, M. Ehara, K. Toyota, R. Fukuda, J. Hasegawa, M. Ishida, T. Nakajima, Y. Honda, O. Kitao, H. Nakai, M. Klene, X. Li, J.E. Knox, H.P. Hratchian, J.B. Cross, C. Adamo, J. Jaramillo, R. Gomperts, R.E. Stratmann, O. Yazyev, A.J. Austin, R. Cammi, C. Pomelli, J.W. Ochterski, P.Y. Ayala, K. Morokuma, G.A. Voth, P. Salvador, J.J. Dannenberg, V.G. Zakrzewski, S. Dapprich, A.D. Daniels, M.C. Strain, O. Farkas, D.K. Malick, A.D. Rabuck, K. Raghavachari, J.B. Foresman, J.V. Ortiz, Q. Cui, A.G. Baboul, S. Clifford, J. Cioslowski, B.B. Stefanov, G. Liu, A. Liashenko, P. Piskorz, I. Komaromi, R.L. Martin, D.J. Fox, T. Keith, M.A. Al-Laham, C.Y. Peng, A. Nanayakkara, M. Challacombe, P.M.W. Gill, B. Johnson, W. Chen, M.W. Wong, C. Gonzalez, J.A. Pople, GAUSSIAN 03, Revision C.01, Gaussian Inc., Wallingford, CT, 2004.
[9] (a) J.S. Binkley, J.A. Pople, W.J. Hehre, J. Am. Chem. Soc. 102 (1980) 939;
(b) M.S. Gordon, J.S. Binkley, J.A. Pople, W.J. Pietro, W.J. Hehre, J. Am. Chem. Soc. 104 (1982) 2797;
(c) W.J. Pietro, M.M. Francl, W.J. Hehre, D.J. DeFrees, J.A. Pople, J.S. Binkley, J. Am. Chem. Soc. 104 (1982) 5039.
[10] (a) W.J. Hehre, R. Ditchfield, J.A. Pople, J. Chem. Phys. 56 (1972) 2257;
(b) P.C. Hariharan, J.A. Pople, Theor. Chim. Acta 28 (1973) 213;
(c) M.S. Gordon, Chem. Phys. Lett. 76 (1980) 163.
[11] (a) P.J. Hay, W.R. Wadt, J. Chem. Phys. 82 (1985) 270;
(b) W.R. Wadt, P.J. Hay, J. Chem. Phys. 82 (1985) 284;
(c) P.J. Hay, W.R. Wadt, J. Chem. Phys. 82 (1985) 299.
[12] P. Flükiger, H.P. Lüthi, S. Portmann, J. Weber, MOLEKEL 4.0, Swiss Center for Scientific Computing, Manno, Switzerland, 2000.
[13] Ö. Farkas, H.B. Schlegel, Phys. Chem. Chem. Phys. 4 (2002) 11.
[14] A.D. Becke, Phys. Rev. A 38 (1988) 3098.
[15] (a) C. Lee, W. Yang, R.G. Parr, Phys. Rev. B: Condens. Matter 37 (1992) 785;
(b) B. Miehlich, A. Savin, H. Stoll, H. Preuss, Chem. Phys. Lett. 157 (1989) 200.
[16] A.D. Becke, J. Chem. Phys. 98 (1993) 5648.
[17] J.P. Perdew, K. Burke, Y. Wang, Phys. Rev. B: Condens. Matter 54 (1996) 16533.
[18] C. Møller, M.S. Plesset, Phys. Rev. 46 (1934) 618.
[19] K.A. Peterson, J. Chem. Phys. 119 (2003) 11099.
[20] (a) V.A. Sipachev, J. Mol. Struct. (Theochem) 121 (1985) 143;
(b) V.A. Sipachev, J. Mol. Struct. 567 (2001) 67.
[21] (a) O. Bastiansen, M. Trætteberg, Acta Crystallogr. 13 (1960) 1108;
(b) Y. Morino, S.J. Cyvin, K. Kuchitsu, T. Iijima, J. Chem. Phys. 36 (1962) 1109;
(c) R. Stølevik, H.M. Seip, S.J. Cyvin, Chem. Phys. Lett. 15 (1972) 263.

[22] C.M. Huntley, G.S. Laurenson, D.W.H. Rankin, J. Chem. Soc., Dalton Trans. (1980) 954.

[23] H. Fleischer, D.A. Wann, S.L. Hinchley, K.B. Borisenko, J.R. Lewis, R.J. Mawhorter, H.E. Robertson, D.W.H. Rankin, Dalton Trans. (2005) 3221.

[24] S.L. Hinchley, H.E. Robertson, K.B. Borisenko, A.R. Turner, B.F. Johnston, D.W.H. Rankin, M. Ahmadian, J.N. Jones, A.H. Cowley, Dalton Trans. (2004) 2469.

[25] A.W. Ross, M. Fink, R. Hilderbrandt, in: A.J.C. Wilson (Ed.), International Tables for Crystallography, vol. C, Kluwer Academic Publishers, Dordrecht, Netherlands, 1992, p. 245.

[26] N. Fey, J. Chem. Technol. Biotechnol. 74 (1999) 852, and references therein.

[27] D.A. Wann, S.L. Hinchley, K.B. Borisenko, H.E. Robertson, M.D. Francis, J.F. Nixon, D.W.H. Rankin, Dalton Trans. (2005) 1972.

[28] (a) A.J. Blake, P.T. Brain, H. McNab, J. Miller, C.A. Morrison, S. Parsons, D.W.H. Rankin, H.E. Robertson, B.A. Smart, J. Phys. Chem. 100 (1996) 12280;
(b) P.T. Brain, C.A. Morrison, S. Parsons, D.W.H. Rankin, J. Chem. Soc., Dalton Trans. (1996) 4589;
(c) N.W. Mitzel, D.W.H. Rankin, Dalton Trans. (2003) 3650.